Substantial Stores of Sedimentary Carbon held in Mid-Latitude Fjords.

C. Smeaton[1], W. E. N. Austin[1,2], A. L. Davies[1], A. Baltzer[3], R. E. Abell[2] and J. A. Howe[2].

[1]{School of Geography & Geosciences, University of St-Andrews, St-Andrews, KY16 9AL, UK}

[2]{Scottish Association for Marine Science, Scottish Marine Institute, Oban PA37 1QA, UK}

[3]{Institut de Géographie et d'Aménagement Régional de l'Université de Nantes, BP 81 227 44312 Nantes cedex 3}

Correspondence to: C. Smeaton (cs244@st-andrews.ac.uk)

Abstract

Quantifying marine sedimentary carbon stocks is key to improving our understanding of long-term storage of carbon in the coastal ocean and to further constraining the global carbon cycle. Here we present a methodological approach which combines seismic geophysics and geochemical measurements to quantitatively estimate the total stock of carbon held within marine sediment. Through the application of this methodology to Loch Sunart a fjord on the west coast of Scotland, we have generated the first full sedimentary carbon inventory for a fjordic system. The sediments of Loch Sunart hold 26.9 ± 0.5 Mt of carbon split between 11.5 ± 0.2 Mt and 15.0 ± 0.4 Mt of organic and inorganic carbon respectively. These new quantitative estimates of carbon stored in coastal sediments are significantly higher than previous estimates. Through an area normalised comparison to adjacent Scottish peatland carbon stocks we have determined that these mid–latitude fjords are significantly more effective as carbon stores than their terrestrial counterparts. This initial work supports the concept that fjords are important environments for the burial and long-term storage of carbon and therefore should be considered and treated as unique environments within the global carbon cycle.

1 Introduction

The rising prominence of Blue Carbon, i.e. carbon (C) which is stored in coastal ecosystems, notably, mangroves, tidal marshes, seagrass meadows and sediments has forced a reassessment of our knowledge of C in the coastal ocean (Nellemann et al., 2009). In recent years there have been a number of reviews (Bauer et al., 2013, Cai et al., 2011, Duarte, 2016) highlighting knowledge gaps and the limited understanding of both the C sources and sinks in the coastal ocean (Bauer et al. 2013). Quantifying the stores of C in the coastal ocean is the first step to a better understanding of coastal carbon dynamics. Global C burial in the coastal zone is estimated in the region of 237.6 Tg yr^{-1} with approximately 126.2 Tg yr^{-1} of C being buried in depositional areas i.e. estuaries and the shelf (Duarte et al., 2005). The lack of regional and national coastal sedimentary C inventories means these global estimates cannot be confirmed or further constrained.

One of the rare examples of a national marine C inventory was carried out by Burrows et al. (2014) producing initial estimates of Blue Carbon in Scottish territorial waters; they calculated that these waters stored 1757 Mt C, with coastal and offshore sediments acting as the main repositories. Burrows et al. (2014) suggested that the majority of this organic carbon (OC) was held in fjord sediments.

It has long been known that fjords are important stores of C (Syvitski et al., 1987) and that C burial in sediments is the most significant mechanism of long-term (>1000years) OC sequestration in the coastal ocean setting (Hedges et al., 1995). These carbon accumulation and burial processes have been investigated in the fjordic systems of New Zealand (Pickrill. 1993, Knudson et al., 2011, Hinojosa et al., 2014, Smith et al.2015), Chile (Sepúlveda et al., 2011), Alaska (Cui et al., 2016) and the high-latitudes of NW Europe (Winkelmann and Knies. 2005, Müller. 2001, Kulinski et al., 2014), yet the mid-latitude fjords of Scotland have been largely overlooked with only limited data available (Loh et al., 2008). Smith et al. (2015) brought much of the available data together and showed that globally fjordic systems act as a CO_2 "buffer" by efficiently capturing and burying labile terrestrially derived OC and preventing it from entering the adjacent ocean system where it is prone to recycling. These authors calculated that 11% of annual global marine carbon sequestration occurs within fjords.

Despite these findings, much of the global research to assess and quantify C stocks is disproportionately skewed towards the terrestrial environment (e.g. Yu et al., 2010). This

trend is also found at the regional scale where there have been multiple studies quantifying the carbon held within Scottish soils (Aitkenhead and Coull 2016, Bradley et al., 2005, Chapman et al., 2013) and peats (Aitkenhead and Coull 2016, Howard et al., 1995, Cannell et al., 1999, Chapman et al., 2009).

In addition to the challenges of access and cost to sample these environments when compared to the adjacent terrestrial environment, it might also be argued that the sparsity of marine sedimentary C inventories is due to the lack of a robust methodology to quantify these C stores. Syvitski et al. (1987) commented that "the development of a methodological approach to quantify the C in the sediment of a fjord must be a priority", yet in the subsequent years there has been relatively little progress towards this goal.

The absence of a robust methodology to quantify the C held in marine sediments is illustrated by Burrows et al. (2014), who estimated that there is 0.34 Mt OC stored in the sediments of Scottish fjords. However, these calculations only take into account an estimate of OC in the top 10 cm of sediment, despite the fact that sediment depths of >25 m are common in Scottish fjords (Baltzer et al., 2010, Howe et al. 2002). Therefore, it is likely that current best estimates (Burrows et al., 2014) of the quantity of OC within these systems as a whole have been significantly underestimated and that the presence of significant quantities of inorganic carbon (IC) held within fjord sediments (Nørgaard-Pedersen et al., 2005) has been overlooked.

This study combines geochemical, geophysical and geochronological techniques to produce a methodology capable of delivering quantitative first-order estimates of the mass of C stored within the sediment of a fjord and, potentially, of achieving the goal set out by Syvitski et al. (1987). This work provides the first carbon inventory for a fjord and further develops the concept of these fjords as being globally important sites for the burial of C as set out by Smith et al. (2015) and Cui et al. (2016b).

2 Material & Methods

2.1 Study Area

Loch Sunart is a fjord on the West coast of Scotland (Fig.1). The fjord is 30.7 km long and covers an area of 47.3 km^2 with a maximum depth of 145 m. It consists of three basins separated by shallower, rock sills. The inner basin is separated from the middle basin by a sill at approximately 6 m depth, while the middle and outer basins are separated by a sill at

approximately 31 m depth (Edwards and Sharples, 1986, Gillibrand et al., 2005). The silled nature of the bathymetry allows the fjord to act as a natural sediment trap for both terrestrial and marine derived materials (e.g. Nørgaard-Pedersen et al., 2006).

Loch Sunart's catchment covers 299 km^2; the main tributaries of the fjord are the Rivers Carnoch and Strontian; the latter has a mean daily discharge of 1409 m^3 (2009-2013). The mean annual precipitation in Loch Sunart's catchment is 2632 ± 262 mm (Capell et al., 2013). The combination of small catchment size and high precipitation means that the flow network is sensitive to precipitation changes which can result in a flashy flow regime (Gillibrand et al., 2005).

The catchment is largely dominated by high relief and poorly developed soils. The bedrock consists primarily of igneous and metamorphic rocks, overlain by gley and podzol soils with limited peat in the upper catchment (Soil Survey of Scotland, 1981). Exposed rock is common on the steep slopes; much of the catchment's vegetation can be found by streams or on the shore of the fjord and is dominated by both commercial forestry and natural woodlands; there is only very limited agriculture within the catchment. The combination of steep, exposed slopes, poorly developed soil, a reactive river network and poorly developed vegetation typically results in high surface runoff and sediment transport (Hilton et al., 2011).

The characteristics of Loch Sunart and its catchment are representative of fjords across mainland Scotland (Edwards and Sharples., 1986), with the possible exception of Loch Etive which has a permanently hypoxic upper basin (Friedrich et al., 2014). The fjords of the Scottish Islands (Shetland, Orkney & the Western Isles) differ from their mainland counterparts in that they are generally shallower and have catchments characterised by lower relief and are largely dominated by peat or peaty soil (Soil Survey of Scotland., 1981). Syvitski and Shaw's (1995) table of generalised fjord characteristics allows us to compare the fjords of mainland Scotland to other fjordic systems globally. The fjords of the Norwegian mainland, Canada and Fiordland, New Zealand (Hinojosa et al., 2014) are characterised by similar climate, geomorphology, river discharge, basin water temperature and sedimentation rate as the fjords of Scotland. The fjords of mainland Scotland differ significantly from those in Greenland, Alaska, Svalbard and the Canadian Arctic, many of which still have active glaciers, resulting in very different sediment input regimes.

2.2 Seismic Data Acquisition and Processing

2.2.1 Data Acquisition

A seismic geophysical survey of Loch Sunart took place in 2002 aboard the RV *Envoy* (Fig.2). A Seistec Boomer System was used to create seismic profile data throughout the fjord. The data were recorded using an Elics-Delph data acquisition system coupled to the Differential Global Positioning System (DGPS). The Boomer system operated on a frequency of 1 to 10 kHz and had a pulse duration of 75 to 250 ms at a power of 150 J. The system has a depth resolution of 25 cm and can penetrate 100 m in soft sediment (Simpkin and Davis. 1983). A total of 34 transects of the fjord were acquired (Fig.2). The survey achieved an average penetration of 50 m; gas blanking prevented the signal from penetrating the sediment in some areas (Baltzer et al., 2010).

2.2.2 Defining Sedimentary Horizons

Each seismic profile was combined with the DGPS data and processed with the Petrel (Schlumberger) software package. Subsequent analysis was undertaken using the open source SeiSee (DMNG) software package. Initial interpolation, following Baltzer et al.'s (2010) methodology, defined the different seismic horizons (H) and the layers between the horizons which are defined as seismic units (U) numbered 1 to 3 from the basement horizon upwards (Fig 3). The compilation of the horizons and units allows the construction of an equivalent seismic stratigraphy for each sediment core and the fjord as a whole.

Using SeiSee, points were picked along each of the four horizons creating polylines. Each polyline was split into points at 0.25 m intervals and each point was assigned an x,y,z coordinate that represents its geographic location and depth (relative to mean sea level).

2.3 Sediment Sampling

Eight sediment cores (Table.1) were collected from Loch Sunart (Fig.1) in 2001 using a gravity corer (GC) as part of the HOLSMEER project. This was supplemented with further sampling on a follow-up cruise on-board the *RV Calanus* in August 2013 where a short GC was collected to fill a gap between the original coring sites. These cores capture the post-glacial history of sediment accumulation within the fjord, as confirmed by ^{14}C basal dates. Additionally, we accessed the lower sections of core MD04 2833 which was recovered using the CALYPSO giant piston corer from the *RV Marion Dufresne* in July 2004 as part of the

IMAGES project. Sampling of Section VIII (1050-1200 cm) of MD04 2833 was undertaken to obtain sediment of inferred glacial origin for geochemical analysis (Baltzer et al., 2010).

2.4 Sediment Analysis

2.4.1 Physical Characteristics

Detailed sediment logging was undertaken for each of the cores (Supplementary Material). The gravity cores were sub-sampled at 10 cm intervals and high resolution sampling at 1 cm intervals was undertaken on the short core (GC01). Section VIII of glacial sediment core MD04-2833 was sub-sampled at 12 cm intervals. Each sub-sample was split for physical property and geochemical analyses. The wet (WBD) and dry bulk density (DBD) of the sediment was calculated following Dadey et al. (1992) while porosity was calculated using the methodology of Danielson and Sutherland. (1986).

2.4.2 Bulk Elemental Analysis

To quantify the total carbon (TC) content, each sub-sample was freeze-dried and milled to a fine powder. A 20 ± 2 mg aliquot was placed in a tin capsule and measured on a COSTECH Elemental Analyser (EA) calibrated with acetanilide (Verardo et al, 1990, Nieuwenhuize et al., 1994). Precision of the analysis is estimated from repeat analysis of standard reference material B2178 (Medium Organic content standard, Elemental Micro analysis, UK) C = 0.07% N = 0.02% (n = 8).

To quantify OC, the process was repeated with the addition of H_2SO_3 to remove the inorganic carbon (IC). After acidification vessels were placed in a vacuum desiccator to remove any remaining CO_2 and the sample was then freeze-dried to remove the H_2SO_3 (Loh et al., 2008). IC was calculated from the difference between TC and OC measurements. The mean standard deviation of TC and OC triplicate measurements (n=10) were 0.04 %, 0.17 % respectively.

2.4.3 Sediment Geochronology

Basal radiocarbon dates for five of the gravity cores were obtained by accelerator mass spectrometer (AMS) radiocarbon dating of marine carbonate material (mollusc). This was carried out at the University of Aarhus, Denmark (AAR), Centre of Accelerator Mass Spectrometry, USA (CAMS) and the NERC Radiocarbon Laboratory, Scotland (SUERC). The radiocarbon dating was used to validate the Holocene chronology of the seismic

stratigraphy. A single MD04-2833 sample was processed at Laval University, Canada (UL) to confirm that the sediment was early post-glacial in age. Dates were calibrated using OxCal 4.2.4 age modelling software (Bronk Ramsey., 2009 & Bronk Ramsey & Lee., 2013) applying the Marine13 curve (Reimer et al., 2013) and the regional marine radiocarbon reservoir age correction: ΔR value of -26 ± 14 yr (Cage et al., 2006).

2.5 Sediment Quantification & Characterisation

2.5.1 Digital Terrain Models (DTM)

The points collected from each seismic horizon were connected to form a DTM of that horizon. This was achieved using spatial modelling techniques in ArcGIS. The compiled *x,y,z* data were statistically tested to determine the gridding technique best suited to the interpolation of the data. Eleven gridding techniques were subjected to cross validation (Chiles and Delfiner 1999)(Supplementary Material). The residual Z mean value and standard deviation were examined; the technique with the lowest residual Z mean and standard deviation for each horizon (and the data set as a whole) was chosen as the gridding technique best suited to the interpolation of the data. Kriging (with linear interpolation) (Cressie, 1990) with a 100 by 1,000 node structure performed best and was chosen to create computationally efficient DTMs for each seismic horizon.

2.5.2 Volumetric Calculations

The horizon DTM grids were used to calculate the volume of sediment in each seismic unit and, by extension, within the fjord as a whole. By subtracting one DTM grid from another (e.g. Surface DTM – Bedrock DTM) the volume between the grids was calculated. Three different numerical integration algorithms were used for this calculation (Eq.1,2,3). The net volume is reported as the mean of these three calculations. In the following formulae Δx represents the grid column spacing, Δy represents the grid row spacing and $G_{i,j}$ represents the grid node value in row i and column j, A_i represents the abscissa (Press et al., 1988).

Trapezoidal Rule

The pattern of coefficients is {1,2,2,2,…,2,2,1}: (1)

$$A_i = \frac{\Delta x}{2}[G_{i,1} + 2G_{i,2} + 2G_{i,3} \cdots + 2G_{i,nCol-1} + G_{i,nCol}]$$

$$Volume \approx \frac{\Delta y}{2}[A_1 + 2A_2 + 2A_3 + \cdots 2A_{nCol-1} + A_{nCol}]$$

Extended Simpson's Rule

The pattern of coefficients is {1,4,2,4,2,4,2,…,4,2,1}: (2)

$$A_i = \frac{\Delta x}{3}\left[G_{i,1} + 4G_{i,2} + 2G_{i,3} + 4G_{i,4} + \cdots + 2G_{i,nCol-1} + G_{i,nCol}\right]$$

$$Volume \approx \frac{\Delta y}{3}\left[A_1 + 4A_2 + 2A_3 + 4A_3 + \cdots + 2A_{nCol-1} + A_{nCol}\right]$$

Extended Simpson's 3/8 Rule

The pattern of coefficients is {1,3,3,2,3,3,2,…,3,3,2,1}: (3)

$$A_i = \frac{3\Delta x}{8}\left[G_{i,1} + 3G_{i,2} + 3G_{i,3} + 2G_{1,4} + \cdots + 2G_{i,NCol-1} + G_{i,nCol}\right]$$

$$Volume \approx \frac{3\Delta y}{8}\left[A_1 + 3A_2 + 3A_3 + 2A_3 + \cdots + 2A_{nCol-1} + A_{nCol}\right]$$

2.5.3 Sediment Mass Quantification

The mean dry bulk density (DBD) for each seismic unit was calculated and assigned to the equivalent seismic unit within each core. The spatial distribution of the DBD for each seismic unit was modelled, again using Kriging (with linear interpolation). The resulting contour plot was integrated with the volumetric model for each seismic unit to calculate the dry mass of the sediment held within that seismic unit. The integration process calculates the volume of sediment held within each of the DBD contours and multiplies that volume with the associated DBD value to calculate the mass of sediment.

2.5.4 Sedimentary Carbon Quantification

The same methodology used to integrate the volume and density data was used to combine bulk elemental data with the sediment dry mass calculations. Mean values for TC, OC and IC in each seismic unit were assigned to the seismic units from the available core data. Kriging (with linear interpolation) was again used to create contour maps representing the quantity of TC, OC and IC in each seismic unit and the mass of sediment held between the contours was multiplied by the percentage of OC and IC quantifying the mass C held within the fjord's sediment. Finally, we calculated how effectively the fjord stores C (C_{eff}) as a depth-integrated average value per km^2 for both the post-glacial and glacial derived sediments. This measure allows the fjord's C stores to be directly compared with other C stores (peatlands, soil, etc.).

2.5.5 Carbon Accumulation and Burial

Sedimentation rates (SR) were calculated as an approximation for the postglacial sediment burial history using basal ages and a linear interpolation to the core top, assuming a contemporary surface. We recognise that the calculations will be crude and do not take into consideration factors such as compaction and possible changes in sedimentation rate through time, but these calculations provide initial insight into the variability of SRs within the fjord and allow first-order C accumulation rates (CARs) to be estimated. The SRs were converted to CARs through the use of Equation 4. The %OC, %IC, bulk density and porosity data used for these calculations were based upon a mean value for the postglacial unit of each dated core.

$$CAR = \%C \times SR \times (porosity - 1) \times bulk\ density \quad (4)$$

As there is no available data on how efficiently OC is buried in the sediment of Scottish sea fjords, burial efficiencies of 64% (Sepúlveda et al., 2005) and 80% (Smith et al., 2015) were used to convert CAR's to CBRs (low and high). For the purposes of this study and in the absence of reliable estimates of burial efficiency, we assume that the IC accumulation rates equal the IC burial rates. These CBR's were, in turn, used to calculate the long-term annual average burial of OC and IC; while potentially very useful, such estimates should be treated with caution.

3 Results

3.1 Seismic Interpretation

3.1.1 Seismic Horizons and Units

Four horizons were identified throughout the fjord (Fig.3): these represent the basement (H1) and the sediment water interface (H4) with two intermediate horizons (H2 & H3). Core stratigraphies (Baltzer et al., 2010) indicates that H2 divides the post-glacial and glacial sediment; while H3 splits the post-glacial sediment into two units. The seismic data displays a fifth horizon between H1 and H2 which is only present in the inner basin and partially in the middle basin. We interpret this as glacial sediment from the Younger Dryas, as confirmed by radiocarbon dating (Baltzer et al., 2010, Mokeddem et al., 2010); for the purposes of this paper, the horizon was amalgamated with H2.

A seismic stratigraphy was developed based on these horizons (Fig.3). U1 is interpreted as glacial sediment based on the observation of the short, discontinuous seismic reflections which are synonymous with poorly sorted material; the unit varies in thickness but never drops below a minimum thickness of 10 m. U2 is found throughout the fjord with an average thickness of 5 to 10 m; the unit drapes over U1. U3 is the uppermost unit and has a homogenous thickness of around 1m; it is characterised by laminated acoustic reflections. Both U2 and U3 are interpreted as post-glacial infill of the fjord; though clear in the seismic geophysics the boundary between U2 and U3 is poorly defined in the sediment lithology (Supplementary Material). Similar patterns in seismic stratigraphy have been observed throughout the west coast of Scotland (Binns et al., 1974a, b, Boulton et al., 1981 and Howe et al., 2002).

We compared our interpretation of the seismic data to the seismic interpretation of Baltzer et al., (2010); this exercise was designed to test the replicability of our interpretation and allow potential uncertainties in the seismic interpolation to be built into our future applications. The comparison identified small differences in the depth of H1 (-0.17 m), H2 (+0.34 m) & H3 (-0.22 m). These differences were integrated into the volumetric calculations as an error term.

3.2 Sediment Geochronology

Calibrated radiocarbon dates for the gravity cores (Table. 2) indicate that these cores are comprised of sediment accumulated during the post-glacial period (Holocene). The age of the deeper basal sediment of MD04-2833 (Section VIII) was confirmed through dating of a mollusc (*Pecten maximus*); the calibrated age was 17041 ± 312 cal BP which, combined with the characteristic glacial core lithology of poorly sorted sedimentary material, indicates that this basal sediment of MD04-2833 was deposited by the retreat of the British ice sheet (BIS) at the end of the last glacial period 13500 to 17000 cal BP (Clark et al., 2010, Scourse et al., 2009, Wilson et al., 2002).

Through comparison of the chronologies to the seismic stratigraphy we can test the interpolation and further constrain the age of each seismic unit. The seismic unit for the equivalent depth of each of the radiocarbon samples has been compiled (Table.2), then compared to the seismic unit that the sample would fall into based on age alone as per the Baltzer et al. (2010) chronostratigraphy. Of the 18 samples tested, 15 have ages which match the appropriate seismic units. Three samples (all from GC023) have ages which are

apparently too young for their corresponding seismic unit; this suggests a possible problem with the dating of this particular core, rather than the interpolation of the seismic geophysics. Close inspection of the seismic profile suggests sediment slumping could be the cause of this dating problem at the core site. This test signifies that our interpolation of the seismic geophysics is accurate and that the chronostratigraphy developed for MD04-2833 (Baltzer et al., 2010) can be applied throughout Loch Sunart. The seismic interpolation and the dated samples confirm that both U2 and U3 are postglacial in origin. We can further constrain the age of the seismic units with U2 representing the early to mid-Holocene and U3 mid to late Holocene in age.

3.3 Sediment Analysis

3.3.1 Bulk Density Measurement

Mean DBD was calculated for U1, U2 and U3 from each core. Figure 4 displays the DBD results, which are arranged to mirror the spatial distribution of the cores, from the inner basin to the outer basin. U1 sediment is characterised by the single section of MD04-2833, which has a mean DBD of 2.19 ± 0.09 g cm^{-3}. This is within the range of other northern hemisphere fjords (Pedersen et al., 2012, Forwick et al., 2010 and Baeten et al., 2010). DBD increases down each core as a result of sediment dewatering in response to compaction. GC011 is the only core where U3 has a higher DBD than U2, most likely due to large quantities of shell in the upper part of the core. U1 has the highest DBD; this reflects both the type of sediment deposited during glacial retreat and long-term compaction over the post-glacial period.

3.3.2 Bulk Elemental Analysis

The mean quantity OC and IC has been calculated for U1, U2 and U3 (Fig.5). Again values for U1 have been calculated using basal sediments of MD04-2833 (Section VIII). Clear trends emerge from these data, with U3 always containing a greater quantity of OC than U2, while the proportion of sedimentary OC generally decreases seawards away from the inner basin. The opposite is true for sedimentary IC, which generally increases seawards away from the inner basin.

3.3.3 Volumetric Modelling

The interpolation of the seismic profiles led to the creation of four DTMs (Supplementary Material) which represent horizons H1 to H4. To determine the accuracy of the models, the DTM for H4 was compared to an existing high-resolution bathymetric model of the fjord (Bates et al. 2004). The coordinates (x,y,z) of key high and low points (n=12) were compared between surveys; the mean divergence between surveys were calculated as x: -0.56 m , y: -0.81 m , z: 0.21 m. Although the H4 DTM slightly negatively offsets the x,y and overestimates the z coordinates of these points, the general location and pattern of these seabed features compare favourably.

The DTMs and numerical integration algorithms were combined to calculate the volume of sediment held within each seismic unit. A further subdivision by basin and according to post-glacial (U2 & U3) and glacial (U1) sediment origin has also been undertaken (Table.3). The fjord as a whole contains a greater volume of glacial (6.00×10^{8} m^3 ± 1.89 %) than post-glacial sediment (5.31×10^{8} m^3 ± 7.39 %). Comparison of the three basins indicates that the middle basin contains the greatest combined (post-glacial + glacial) volume of sediment (3.04×10^{7} m^3 ± 5.30 %) followed by the outer (1.60×10^{7}.2 m^3 ± 5.74 %) and inner basins (4.17×10^{6} m^3 ± 4.48 %).

3.3.4 Sediment Mass Quantification

The mean DBD for U2 and U3 were modelled (Fig.6) to determine the variability in spatial distribution throughout the fjord. A similar spatial pattern of DBD is found in both U2 and U3; the DBD is lowest in the inner basin (U2: 0.47 g cm^{-3}, U3: 0.59 g cm^{-3}) rising through the middle basin where it peaks at 1.75 g cm^{-3} and 1.67 g cm^{-3} for U2 and U3 respectively. The transition between the middle and outer basins is characterised with low DBD values (U2: 0.72 g cm^{-3}, U3: 0.91 g cm^{-3}); from this low point the DBD rises towards the seaward end of the fjord.

The model output was integrated with the volumetric data to calculate the mass of sediment held within the post-glacial sequences (Table 4). Since we have a single mean value for DBD for U1 we applied this throughout the fjord to calculate the mass of sediment held within this unit. The fjord holds a total of 1928.3 ± 7.3 Mt of sediment which is split into 652.1 ± 6.6 Mt of post-glacial and 1276.2 ± 8.9 Mt of glacial sediment. The inner basin holds the least

sediment followed by the outer basin with the middle basin acting as the main store of sediment in Loch Sunart.

3.3.5 Sedimentary Carbon Quantification

Using a similar approach, the mean OC and IC were spatially modelled throughout the fjord. The output for U3 is illustrated in Figure 7. As before, the model outputs for U2 and U3 were integrated with the sediment mass data in order to quantify the mass of TC, OC and IC held within the post-glacial and glacial sediments (Table.4). Single mean values for TC, OC and IC were again used to calculate their respective mass of C within the sediment of U1.

The sediment of Loch Sunart holds a significant quantity of C (26.9 ± 0.5 Mt) split between OC (11.5 ± 0.2 Mt) and IC (15.0 ± 0.4 Mt). Though a greater mass of sediment is held within the glacial component, it is the post-glacial sediments which hold the largest quantity of C (19.9 ± 0.3 Mt). The quantity of C held within each of Loch Sunart's basins varies; the lowest amount is found in the inner basin (2.1 ± 0.5 Mt), followed by the outer basin (6.7 ± 0.6 Mt). The sediment of middle basin holds significantly more C than both the inner and outer basins combined; with 18.1 ± 0.7 Mt C stored in these sediments, indicating that the middle basin is the main repository for sedimentary C in Loch Sunart.

How effectively the fjord stores C is measured by the C_{eff} (Table.5) and the OC:IC ratio. Loch Sunart is characterised by an OC:IC ratio of 0.74 and has an average C_{eff} of 0.560 Mt C km^{-2}, which can be further broken down to a post-glacial C_{eff} of 0.412 Mt C km^{-2} and a glacial C_{eff} of 0.148 Mt C km^{-2}. The effective C storage can also be illustrated at the individual basin level with the post-glacial sediments of the inner, middle and outer basins characterised by OC:IC ratios of 4, 1 and 0.42, illustrating the transition from OC as the dominant component of the sediment in the upper fjord to an IC-dominated sediment at the seaward end of the fjord. The middle basin is the most effective at storing post-glacial OC followed by the inner and outer basin; similarly the middle basin is most effective at storing IC, but in contrast to the effective storage of OC, the outer basin ranks second followed by the inner basin for IC. The glacial material held within the fjord as a whole is characterised by an OC:IC ratio of 0.42 with a mean OC_{eff} 0.044 Mt km^{-2} and IC_{eff} 0.104 Mt km^{-2}.

3.3.6 Carbon Accumulation and Burial

The SRs vary between the sedimentary basins of the fjord, with the most rapid rates in the inner basin recorded in core GC013 (0.087 cm yr^{-1}). The middle and outer basins have lower SRs as shown by cores GC020 (0.025 cm yr^{-1}) and GC011 (0.017 cm yr^{-1}). The calculated CARs and CBRs for Loch Sunart are presented in Table. 6 alongside rates from other fjords globally. Our estimates are in-line with the fjords of New Zealand (Pickrill. 1993, Knudson et al., 2011, Hinojosa et al., 2014, Smith et al., 2015), Alaska (vegetated) (Cui et al., 2016) and Chile (Sepúlveda et al., 2011); they are somewhat lower than the glaciated fjords of NW Europe (Winkelmann and Knies 2005, Müller. 2001, Kulinski et al., 2014). Although not shown in Table 6, the calculated ICARs range between 0.69 and 36.89 g IC m^{-2} yr^{-1}, resulting in long-term annual average estimates of IC burial of between 56 and 1.7 x 10^3 tonnes for the fjord as a whole.

3.4 A Methodology for Estimating Sedimentary Carbon and Attributing Uncertainty Estimates

The joint geophysical and geochemical methodology outlined (Fig.8) provides a robust approach to allow the first quantification of total sedimentary C stocks in a fjord setting. An important part of estimating sedimentary C stocks should be the quantification of uncertainty associated with these estimates. There are several types of uncertainty that can influence sedimentary carbon estimations (Fig.8), including interpolation, algorithmic, analytical, sampling and extrapolation uncertainty. Several of these types of uncertainties are easily dealt with statistically, for example the analytical uncertainties have been quantified through triplicate measurements. The sampling uncertainty of a stratigraphic sequence (i.e. spatial variability of C content in relation to sampling density) can be overcome by calculating the mean and standard deviation to create composite values that are representative of the seismic unit as a whole. We integrated the quantifiable uncertainties at each calculation step (Fig.8). By calculating composite standard deviations we are able to propagate the uncertainties throughout the C quantification process. In the interpolation of the seismic geophysics, it is difficult to fully quantify the uncertainty involved in the process. Bond et al. (2007) set out a 5 step framework designed to reduce uncertainty in this process. We utilised the framework of Bond et al. (2007) and additionally integrated a validation step using radiocarbon dating of sedimentary cores (See Section 3.2). This allows us to reduce the uncertainties associated

with the seismic interpretation, although we recognise that some uncertainty remains (e.g. highly variable patterns of sediment thickness) which cannot be fully quantified. Within this framework of uncertainty, we consider our method to give a robust estimate for the carbon stocks present.

4 Discussion: A new Sedimentary C Inventory for Scottish Coastal Waters

The development of this methodology has allowed the estimation of the sedimentary C stocks stored in a mid-latitude fjord. An estimated 26.9 ± 0.5 Mt C has been accounted for within our study site (Loch Sunart).

The only directly comparable estimation for sedimentary C stocks is the report by Burrows et al. (2014), where they calculated that 0.3 Mt OC was stored in all 110 Scottish fjords. In comparison, our findings estimate that Loch Sunart alone holds 11.5 Mt OC. However, Burrows et al. (2014) focused on the top 10 cm of sediment because data availability and the lack of a robust methodology made it impossible to calculate the entire sedimentary C stock; this has resulted in a significant underestimation of the quantity of C held within the sediment of these fjords. Additionally, Borrows et al. (2014) did not consider IC to be a major component in these sediments; instead the authors focused on Scottish fjords largely as OC stores. In contrast, our results demonstrate that Loch Sunart stores 15.0 Mt IC in comparison to 11.5 Mt OC. The general lack IC data for the coastal environment makes it difficult to assess how representative Loch Sunart is of these coastal sedimentary IC stores; however, our results do highlight the potential significance of IC as a major component of sedimentary C stores in these depositional environments. Our results also highlight that fjords in general (Smith et al., 2015) act as an OC rich sediment transition zone between terrestrial and oceanic environments.

Loch Sunart's sediment currently holds 11.5 Mt OC with an additional estimated range of between 89 to 1.2 $x10^3$ tonnes of OC buried annually. This highly localized OC trapping in the coastal zone may further reduce reworking and remineralisation of the material which would have otherwise resulted in the release of CO_2 through biotic processes (Smith et al., 2015). This 11.5 Mt of sedimentary OC is equivalent to 40.9 Mt CO_2e (carbon dioxide equivalent). As a whole, the sediment within Loch Sunart stores 99.6 Mt CO_2e which is equivalent to over two years of Scotland's total greenhouse gas emission for 2014 which reached an estimated 46.7 Mt CO_2e (Scottish Government, 2016).

Globally, the terrestrial C stores have received much more attention than their marine counterparts; with significant focus on quantifying the forest (Köhl et al., 2015) and soil C stocks (Köchy et al., 2015, Scharlemann et al., 2014). The work by Duarte et al. (2005) to compile the known stocks and burial rate of C in the coastal environment highlighted that the coastal ocean constitutes a large store of carbon, which remains poorly understood; from this work the concept of Blue Carbon arose (Nellemann et al., 2009). The focus of Duarte et al. (2005) was to highlight that the vegetated coastal zones (i.e. saltmarsh, seagrass and mangroves) bury and store significant quantities of C and that these stores should be further investigated and recognised in policy outputs, but these authors largely overlook the importance of what they described as depositional area (estuaries and the shelf sea) as long-term repositories of OC detritus from the vegetated coastal environment (Krumhansl et al., 2012) and ignored the terrestrial OC inputs. These authors recognised that coastal (and shelf) depositional areas are important stores of sedimentary C globally, yet almost no consideration is given to how these areas vary in terms of their capacity to store C.

Furthermore, if we consider the range of estuarine environments (e.g. fjord, delta, coastal plain, bar-built and tectonic), it is clear that the characteristics of each type of estuary will impact the manner in which C is buried and stored. For example, the restricted nature of fjords will be conducive to sediment capture and effective C storage when compared to the more open estuarine environments which experience greater flushing. Globally, the rates at which fjords accumulate and bury OC is reasonably well defined (Table. 6). This study adds data for the underrepresented mid-latitude fjords which are comparable to other vegetated fjordic systems around the world (Pickrill. 1993, Sepúlveda et al., 2011, Knudson et al., 2011, Hinojosa et al., 2014, Smith et al., 2015). Additionally, for the first time, we cautiously report IC accumulation and burial rates for a fjord. The burial of IC is another significant mechanism of CO_2 sequestration that has been overlooked in fjordic systems and requires further investigation to quantify its importance to the coastal C cycle as a whole.

Our initial work suggests that the depositional area category could be further expanded upon to include fjords as a separate component and this concept is supported by Smith et al. (2015), who indicated that fjords are “hot-spots for OC burial” and should be considered separately from estuaries when investigating global ocean OC burial. Currently, there is insufficient globally available data to advocate fjords being categorised as a separate component in global

coastal C stores; however, the standardised methodology outlined (Fig.8) provides a platform to investigate this concept further.

At the national level there has been a significant focus on quantifying Scottish soil C stocks, with much attention given to the peatlands (Aitkenhead and Coull. 2016, Bradley et al., 2005 and Chapman et al. 2009). Peat and other organic rich soils cover 66% of Scotland and account for 50% of all the United Kingdom's soil C stocks (Cummins et al., 2011). The Scottish peatlands store 1620 Mt C (Chapman et al., 2009) over an area of 17270 km^2, while the other soils hold 2110.9 Mt C over 60215 km^2 (Aitkenhead and Coull. 2016). In comparison to these figures, the quantity of C stored in Loch Sunart is small, but the fjord itself only covers an area of 47.3 km^2. When the fjord's C_{eff} is compared to how effectively Scotland's soils and peatlands store C (Table. 5), we can see that when normalised as a store per unit area basis Loch Sunart stores significantly more C than the soils of Scotland. The fjord has a C_{eff} of 0.568 Mt C km^{-2} compared to 0.094 Mt C km^{-2} and 0.035 Mt C km^{-2} for the peatlands and other soils of Scotland. Our results suggest that Loch Sunart is one of the most effective stores of C in Scotland and highlights the potential of the sediment in these mid-latitude fjords to hold a significant quantity of C. Many of these terrestrial C stores are, of course, vulnerable to rapid and long-term environmental change; the Scottish terrestrial C stocks are at risk from erosion (Cummins et al. 2011) and even fire (Davies et al., 2013), both of which are increasing in pace and frequency by anthropogenic activities. In comparison, a fjord's geomorphology combined with its depth gives sedimentary C stores a level of protection not afforded to terrestrial C stores. This does not mean that the sedimentary C in sea lochs is invulnerable, but rather that it is buffered from the immediate effects of chemical, biological and physical environmental change during interglacial periods. Over longer timeframes it is known that these sedimentary stores are scoured by glacial advances resulting in the material being transported to the adjacent shelf and slope (Jaeger and Koppes., 2016). Further investigation is required to better understand the processes governing the transfer of material to the shelf and what impact this has on the quality of OC in coastal sediment stores (Smith et al., 2015).

The methodology outlined in this paper provides a platform from which to calculate the carbon stocks in other fjordic systems as well as environments with restricted sediment exchange processes, such as estuaries and freshwater lakes, as well as artificial systems such as reservoirs and irrigation pools.

5 Conclusion

The integration of the geochemical and geophysical techniques outlined provides a robust and repeatable methodology to quantitatively calculate the volume of sediment and make first order estimations of carbon stored within fjordic sediments. Using this methodology we have shown that Loch Sunart, a fjord on the west coast of Scotland holds 26.9 Mt C which is equivalent to double Scotland's CO_2 emissions for 2014. While these individual fjord stores may be small in comparison with Scotland's peatland and soil C stocks, we show they are potentially far more effective stores of both OC and IC than Scotland's terrestrial habitats (area normalised comparison). The results from this study suggest that the sediment in Scotland's 110 fjords (Edwards and Sharples. 1986) represent a potentially significant, yet currently largely unaccounted for repository of both OC and IC. These fjords act to trap sediment and reduce the remineralisation of OC into the atmosphere. Additionally, the C held within these 110 fjords is likely to represent a significant portion of Scotland's blue carbon capital that has not yet been considered at the marine ecosystem, global C cycle and wider policy levels. Without a better understanding of these globally significant stores of marine sedimentary C it remains difficult to fully quantify the coastal C cycle. However, evidence suggests that these fjordic environments do play an important role in buffering the release of CO_2 through the effective burial of large quantities of C in these sediments. The future strategic application of the methodology outlined in this study to different fjord types and locations offers the potential through appropriate upscaling to estimate the fjordic sedimentary C stores both at regional, national and global scales.

Author Contribution

CS & WA conceived the research and wrote the manuscript, to which all co-authors contributed data or provided input. CS conducted the research as part of his PhD at the University of St Andrews, supervised by WA, AD and JH.

Acknowledgements

This work was supported by the Natural Environment Research Council [Grant Number: NE/L501852/1] with additional support from the NERC Radiocarbon Facility [Allocation 1934.1015]. Seismic profiles and the CALYPSO long core were acquired within the frame of the French ECLIPSE program with additional finicial support from NERC, SAMS and the University of St-Andrews. The authors would like to thank Marion Dufresne's Captain J.-M. Lefevre, the Chief Operator Y. Balut (from IPEV) and Richard Bates (University of St

Andrews). Additionally; we would like to thank Colin Abernethy (Scottish Association of Marine Science) for laboratory support. Finally, we thank Jessica Hinojosa and one anonymous reviewer whose insightful comments improved this manuscript.

References

Aitkenhead, M. J. and Coull, M. C.: Mapping soil carbon stocks across Scotland using a neural network model, Geoderma, 262, 187–198, doi:10.1016/j.geoderma.2015.08.034, 2016.

Baeten, N. J., Forwick, M., Vogt, C. and Vorren, T. O.: Late Weichselian and Holocene sedimentary environments and glacial activity in Billefjorden, Svalbard, Geol. Soc. London, Spec. Publ., 344(1), 207–223, doi:10.1144/SP344.15, 2010.

Baltzer, A., Bates, C.R., Mokeddem, Z., Clet-Pellerin, M., Walter-Simonnet, A-V., Bonnot Courtois, C. and Austin, W.E.N. Using seismic facies and pollen analyses to evaluate climatically driven change in a Scottish sea loch (fjord) over the last 20 ka, Geological Society, London, Special Publications, 344, (1), pp. 355–369, 2010

Bauer, J.E., Cai, W-J, Raymond, P.A,, Bianchi, T.S., Hopkinson, C.S., and Regnier, P.A.G. 2013, The changing carbon cycle of the coastal ocean., Nature, 504, (7478), pp. 61–70, 2013

Bates, C.R., Moore, C.G., Harries, D.B., Austin, W.E.N., and Lyndon, A. R. Broad scale mapping of sublittoral habitats in Loch Sunart, Scotland. Scottish Natural Heritage Commissioned. Report No. 006 (ROAME No. F01AA401C), 2004.

Binns, P. E., Harland,R. & Hughes, M. J. 1974a. Glacial and post glacial sedimentation in the sea of the Hebrides. Nature, 248, 751–754, 1974a.

Binns, P. E., Mcquillin,R.& Kenolty, N. 1974b. The geology of the sea of the Hebrides. Institute of Geological Sciences 73/14, 1974b.

Boulton, G. S., Chroston,P.N.& Jarvis, J. A marine seismic study of late Quaternary sedimentation and inferred glacier fluctuations along western Inverness–shire, Scotland. Boreas, 10, 39–51, 1981.

Bond, C. E., Gibbs, A. D., Shipton, Z. K. and Jones, S.: What do you think this is? "Conceptual uncertainty" In geoscience interpretation, GSA Today, 17(11), 4–10, doi:10.1130/GSAT01711A.1, 2007.

Bradley, R.I., Milne, R., Bell, J., Lilly, A.., Jordan, C. and Higgins, A.: A soil carbon and land use database for the United Kingdom. Soil Use and Management, 21, 363–369, 2005

Bronk Ramsey, C. Bayesian analysis of radiocarbon dates. Radiocarbon, 51(1), 337-360, 2009

Bronk Ramsey, C. and Lee, S. Recent and planned developments of the program OxCal. Radiocarbon, 55(2-3), 720-730, 2013

Burrows M.T., Kamenos N.A., Hughes D.J., Stahl H., Howe J.A. and Tett P. Assessment of carbon budgets and potential blue carbon stores in Scotland's coastal and marine environment. Scottish Natural Heritage Commissioned Report No. 761, 2014

Cage, A.G., Heinemeier, J. and Austin, W.E.N. Marine radiocarbon reservoir ages in Scottish coastal and fjordic waters, Radiocarbon, Vol 48, Nr 1, 31–43, 2006.

Cai, W.-J.: Estuarine and coastal ocean carbon paradox: CO2 sinks or sites of terrestrial carbon incineration?, Ann. Rev. Mar. Sci., 3, 123–45, doi:10.1146/annurev-marine-120709-142723, 2011.

Capell, R., Tetzlaff, D. and Soulsby, C.: Will catchment characteristics moderate the projected effects of climate change on fl ow regimes in the Scottish Highlands ?, , 699(December 2012), 687–699, doi:10.1002/hyp.9626, 2013.

Cannell, M.G.R., Milne, R., Hargreaves, K.J., Brown, T.A.W., Cruickshank, M.M., Bradley, R.I., Spencer, T., Hope, D., Billett, M.F., Adger, W.N. and Subak, S. National inventories of terrestrial carbon sources and sinks: The UK experience. Climatic Change, 42, 505–530, 1999

Clark, C. D., Hughes, A. L. C., Greenwood, S. L., Jordan, C. and Petter, H.: Pattern and timing of retreat of the last British-Irish Ice Sheet, Quat. Sci. Rev., doi:10.1016/j.quascirev.2010.07.019, 2010.

Chapman, S.J., Bell, J.S., Campbell, C.D., Hudson, G, Lilly, A., Nolan, A.J., Robertson, A.H.J., Potts, J.M., and Towers, W, Comparison of soil carbon stocks in Scottish soils between 1978 and 2009, European Journal of Soil Science, 64, (4), pp. 455–465, 2013

Chapman, S.J., Bell, J., Donnelly, D. and Lilly, A., Carbon stocks in Scottish peatlands, Soil Use and Management, 25, (2), pp. 105–112, 2009.

Chiles, J.P., and Delfiner.P. Geostatistics: Modeling Spatial Uncertainty. John Wiley and Sons, New York, 695, 1999.

Cressie, N.A.C. The Origins of Kriging, Mathematical Geology, v. 22, p. 239-252, 1990.

Cui, X., Bianchi, T. S., Jaeger, J. M. and Smith, R. W.: Biospheric and petrogenic organic carbon flux along southeast Alaska, Earth Planet. Sci. Lett., 452, 238–246, doi:10.1016/j.epsl.2016.08.002, 2016.

Cui, X., Bianchi, T. S., Savage, C. and Smith, R. W.: Organic carbon burial in fjords : Terrestrial versus marine inputs, Earth Planet. Sci. Lett., 451, 41–50, doi:10.1016/j.epsl.2016.07.003, 2016b.

Cummins, R., Donnelly, D., Nolan, A., Towers, W., Chapman, S., Grieve, I. and Birnie, R.V. Peat erosion and the management of peatland habitats. Scottish Natural Heritage Commissioned Report No. 410, 2011

Dadey, K.A., Janecek, T. and Klaus, A Dry bulk density: its use and determination, Proceedings of the Ocean Drilling Program, Scientific Results, Vol. 126, 1992.

Danielson, R.E., Sutherland, P.L.,Porosity. In: Klute, A. (eds),Methods of soil analysis, part 1, Physical and mineralogical methods, Am. Soc. Agr., Madison, Wisconsin, pp. 443–461. 1986.

Davies, G. M., Gray, A., Rein, G. and Legg, C. J.: Peat consumption and carbon loss due to smouldering wildfire in a temperate peatland, For. Ecol. Manage., 308, 169–177, doi:10.1016/j.foreco.2013.07.051, 2013.

Duarte, C. M., Middelburg, J. J. and Caraco, N.: Major role of marine vegetation on the oceanic carbon cycle, Biogeosciences, 2, 1–8, 2005.

Duarte, C. M.: Reviews and syntheses : Hidden Forests , the role of vegetated coastal habitats on the ocean carbon budget, , 1981(August), 1–17, doi:10.5194/bg-2016-339, 2016.

Edwards,A.& Sharples, F. Scottish Sea Lochs: A Catalogue. Scottish Marine Biological Association/ Nature Conservancy Council, Oban, 1986.

Forwick, M., Vorren, T. O., Hald, M., Korsun, S., Roh, Y., Vogt, C. and Yoo, K.-C.: Spatial and temporal influence of glaciers and rivers on the sedimentary environment in Sassenfjorden and Tempelfjorden, Spitsbergen, Geol. Soc. London, Spec. Publ., 344(1), 163–193, doi:10.1144/SP344.13, 2010.

Friedrich, J., Janssen, F., Aleynik, D., Bange, H. W., Boltacheva, N., Çagatay, M. N., Dale, a. W., Etiope, G., Erdem, Z., Geraga, M., Gilli, a., Gomoiu, M. T., Hall, P. O. J., Hansson, D., He, Y., Holtappels, M., Kirf, M. K., Kononets, M., Konovalov, S., Lichtschlag, a., Livingstone, D. M., Marinaro, G., Mazlumyan, S., Naeher, S., North, R. P., Papatheodorou, G., Pfannkuche, O., Prien, R., Rehder, G., Schubert, C. J., Soltwedel, T., Sommer, S., Stahl, H., Stanev, E. V., Teaca, a., Tengberg, a., Waldmann, C., Wehrli, B. and Wenzhöfer, F.:

Investigating hypoxia in aquatic environments: Diverse approaches to addressing a complex phenomenon, Biogeosciences, 11(4), 1215–1259, doi:10.5194/bg-11-1215-2014, 2014.

Gillibrand, P.A., Cage, A.G. and Austin, W.E.N. A preliminary investigation of basin water response to climate forcing in a Scottish fjord: evaluating the influence of the NAO, Continental Shelf Research, 25, (5-6), pp. 571–587, 2005

Hedges, J.I., Keil, R.G. and Benner, R. What happens to terrestrial organic matter in the ocean? Organic Geochemistry. 27, 195–212, 1997.

Hilton, R.G., Galy, A., Hovius, N. & Horng, M.J. Efficient transport of fossil organic carbon to the ocean by steep mountain rivers: An orogenic carbon sequestration mechanism. Geology 39, 71–74, 2011.

Hinojosa, J.L, Christopher M. Moy, C.M, Claudine H. Stirling, C.H, Gary S. Wilson, G.S, and Eglinton, T.I : Carbon cycling and burial in New Zealand's fjords, , 4047–4063, doi:10.1002/2014GC005433.Received, 2014.

Howard, P.J.A., Loveland, P.J., Bradley, R.I., Dry, F.T., Howard, D.M. and Howard, D.C.. The carbon content of soil and its geographical distribution in Great Britain. Soil Use and Management, 11, 9–15, 1995.

Howe, J. A., Shimmield, T., Austin, W. E. N. and Longva, O.: Post-glacial depositional environments in a mid-high latitude glacially-overdeepened sea loch , inner Loch Etive , western Scotland, , 185, 417–433, 2002.

Jaeger, J. M. and Koppes, M. N.: The role of the cryosphere in source-to-sink systems, Earth-Science Rev., 153, 43–76, doi:10.1016/j.earscirev.2015.09.011, 2016.

Johnston, D.H and R. Cooper, M.R., Methods and Applications in Reservoir Geophysics, Investigations in geophysics, no. 15., Tulsa, OK : Society of Exploration Geophysicists, 2010.

Kennedy, P., Kennedy, H., and Papadimitriou, S. The effect of acidification on the determination of organic carbon, total nitrogen and their stable isotopic composition in algae and marine sediment, Rapid Communications in Mass Spectrometry, 19, (8), pp. 1063–1068, 2005.

Knudson, K. P., Hendy, I.L. and Neil, H.L.: Re-examining Southern Hemisphere westerly wind behaviour: Insights from a late Holocene precipitation reconstruction using New Zealand fjord sediments, Quat. Sci. Rev., 30(21-22), 3124–3138, doi:10.1016/

j.quascirev.2011.07.017, 2011.Köchy, M., Hiederer, R. and Freibauer, A.: Global distribution of soil organic carbon – Part 1: Masses and frequency distributions of SOC stocks for the tropics, permafrost regions, wetlands, and the world, Soil, 1(1), 351–365, doi:10.5194/soil-1-351-2015, 2015.

Köhl, M., Lasco, R., Cifuentes, M., Jonsson, ??rjan, Korhonen, K. T., Mundhenk, P., de Jesus Navar, J. and Stinson, G.: Changes in forest production, biomass and carbon: Results from the 2015 UN FAO Global Forest Resource Assessment, For. Ecol. Manage., 352, 21–34, doi:10.1016/j.foreco.2015.05.036, 2015

Krumhansl, K. A. and Scheibling, R. E.: Production and fate of kelp detritus, Mar. Ecol. Prog. Ser., 467, 281–302, doi:10.3354/meps09940, 2012.

Kuliński K, Kędra M, Legeżyńska J, Głuchowska M, Zaborska A, Particulate organic matter sinks and sources in high Arctic fjord. J Mar Syst 139:27–37, 2014.

Mokeddem, Z., Baltzer, A.., Goubert, E and Clet-Pellerin, M., A multiproxy palaeoenvironmental reconstruction of Loch Sunart (NW Scotland) since the Last Glacial Maximum, Geological Society, London, Special Publications, 344, (1), pp. 341–353, 2010.

Müller, A., Geochemical expressions of anoxic conditions in Nordåsvannet, a land-locked fjord in western Norway Appl. Geochem., 16, pp. 363–374, 2001.

Nellemann C., Corcoran E., Duarte C.M., Valdés L., DeYoung C., Fonseca L., Grimsditch G. (Eds.), Blue Carbon: A Rapid Response Assessment, United Nations Environment Programme, GRID-Arendal, (2009).

Nieuwenhuize, J., Maas, Y.E.M., and Middelburg, J.J. Rapid analysis of organic carbon and nitrogen in particu- late materials. Mar. Chem. 45:217-224, 1994

Nørgaard-Pedersen, N., Austin, W. E. N., Howe, J. a. and Shimmield, T.: The Holocene record of Loch Etive, western Scotland: Influence of catchment and relative sea level changes, Mar. Geol., 228(1-4), 55–71, doi:10.1016/j.margeo.2006.01.001, 2006.

Pedersen, J. B. T., Kroon, a., Jakobsen, B. H., Mernild, S. H., Andersen, T. J. and Andresen, C. S.: Fluctuations of sediment accumulation rates in front of an Arctic delta in Greenland, The Holocene, 23(6), 860–868, doi:10.1177/0959683612474480, 2013.

Pergamon Press, 119–41Polson, D. and Curtis, A.: Dynamics of uncertainty in geological interpretation, J. Geol. Soc. London., 167(1), 5–10, doi:10.1144/0016-76492009-055, 2010.

Press, W.H., Flannery, B.P., Teukolsky, S.A., and Vetterling, W.T. Numerical Recipes in C, Cambridge University Press, 1988.

Pickrill, R. A., Sediment yields in Fiordland, J. Hydrol. N. Z., 31(1), 39–55, 1993.

Reimer, P, IntCal13 and Marine13 Radiocarbon Age Calibration Curves 0–50,000 Years cal BP, Radiocarbon, 55, (4), pp. 1869–1887, 2013.

Scottish Government. 2016. http://www.gov.scot/Publications/2016/06/2307; Accessed 09/09/2016.

Scharlemann, J. P., Tanner, E. V., Hiederer, R. and Kapos, V.: Global soil carbon: understanding and managing the largest terrestrial carbon pool, Carbon Manag., 5(1), 81–91, doi:10.4155/cmt.13.77, 2014.

Scourse, J. D., Haapaniemi, A. I., Colmenero-hidalgo, E., Peck, V. L., Hall, I. R., Austin, W. E. N., Knutz, P. C. and Zahn, R.: Growth , dynamics and deglaciation of the last British – Irish ice sheet : the deep-sea ice-rafted detritus record, Quat. Sci. Rev., 28(27-28), 3066–3084, doi:10.1016/j.quascirev.2009.08.009, 2009

Sepúlveda, J., Pantoja, S., Hughen, K., Lange, C., Gonzalez, F., Muñoz, P., Rebolledo, L., Castro, R., Contreras, S., Ávila, A., Rossel, P., Lorca, G., Salamanca, M. and Silva, N.: Fluctuations in export productivity over the last century from sediments of a southern Chilean fjord (44°S), Estuar. Coast. Shelf Sci., 65(3), 587–600, doi:10.1016/j.ecss.2005.07.005, 2005.

Sepúlveda, J.., Pantoja, S., Hughen. K.A.,: Sources and distribution of organic matter in northern Patagonia fjords, Chile (44–47°S): A multi-tracer approach for carbon cycling assessment, Cont. Shelf Res., 31(3-4), 315–329, doi:10.1016/j.csr.2010.05.013, 2011.

Simpkin,P.G. and Davis, A, For seismic profiling in very shallow water, a novel receiver. In Sea Technology, 1983.

Smith, R.W., Bianchi, T,S., Allison, M., Savage, C. & Galy, V, High rates of organic carbon burial in fjord sediments globally, Nature, doi: 10.1038/NGEO2421, 2015.

Soil Survey of Scotland Staff. (1970-1987). Soil maps of Scotland (partial coverage) at a scale of 1:25 000. Macaulay Institute for Soil Research, Aberdeen.

St-Onge, G., and Hillaire-Marcel, C.: Isotopic constraints of sedimentary inputs and organic carbon burial rates in the Saguenay Fjord, Quebec, Mar. Geol., 176(1-4), 1–22, doi:10.1016/S0025-3227(01)00150-5, 2001

Syvitski, J.P.M, Burrell, D.C & Skei, J.M. Fjords, Processes and Products, Springer-Verlag New York, 1987.

Syvitski, J.P.M & Shaw, J: Sedimentology and Geomorphology of Fjords, Geomorphology and Sedimentology of Estuaries. Developments in Sedimentology 53, 1995.

Wilson, L. J., Austin, W. E. N. and Jansen, E.: The last British Ice Sheet : growth , maximum extent and deglaciation, , (2001), 243–250, 2002.

Winkelmann, D. and Knies, J,:Recent distribution and accumulation of organic carbon on the continental margin west off Spitsbergen, Geochem. Geophys. Geosyst., 6, Q09012, doi:10.1029/2005GC000916. 2005

Verardo, D.J., P. N. Froelich, P.N. and McIntyre, A,Determination of organic carbon and nitrogen in marine sediments using the Carlo Erba NA-1500 Analyzer. Deep Sea Res. 37:157-165, 1990

Yu, Z, Loisel, J., Brosseau, D.P., Beilman, D.W., & Hunt, S.J. Global peatland dynamics since the Last Glacial Maximum. Geophysical Research Letters 37, L13402**,** 2010.

Table. 1. Details of the sediment cores extracted from Loch Sunart that were used in this study.

Core ID	Basin	Position (Lat, Long)	Water Depth (m)	Recovery (m)
GC009	Middle	56.672056, -5.867083	107	1.41
GC011	Outer	56.759861, -5.969639	91	2.45
GC013	Inner	56.681306, -5.629528	58	1.67
GC016	Inner	56.680944, -5.642333	58	0.56
GC020	Middle	56.704278, -5.751333	105	2.38
GC022	Middle	56.680333, -5.804944	120	2.46
GC023	Middle	56.665917, -5.840361	87	2.89
GC081	Middle	56.668972, -5.863278	58	3.63
GC01	Middle	56.696806, -5.704972	42	0.21
MD04 2833	Middle	56.665500, -5.859667	38	12

Table. 2 Radiocarbon ages from Loch Sunart cores. Ages were calibrated using OxCal 4.2.4 (Bronk Ramsey., 2009 & Bronk Ramsey & Lee., 2013) with the Marine13 curve (Reimer et al. 2013) and regional correction of ΔR value of -26 ± 14 yr (Cage et al. 2006) . All ages are calibrated at 95.4% probability and the mean age has been determined from the minimum and maximum calibrated ages. Additionally; we list the seismic unit assigned to each equivalent (eqv.) depth and compare this to the age equivalent seismic unit based on Baltzer et al. (2010).

Laboratory Code	**Core ID**	**Depth** (cm)	**^{14}C Age, BP** (No Correction)	**Calibrated ^{14}C Age** (cal BP)	**Seismic Unit**	
					Depth eqv.	**Age eqv.**
AA-48108	GC009	140	9827 ± 49	10801 ± 93	U2	U2
SUERC 65990	GC011	60	2837 ± 35	2625 ± 66	U3	U3
SUERC 65991	GC011	120	9890 ± 38	10878 ± 87	U2	U3
SUERC 65992	GC011	170	11266 ± 40	12760 ± 61	U2	U2
AA-48109	GC011	231	12181 ± 58	13658 ± 90	U1	U1
AA-48107	GC013	113	1716 ± 32	1294 ± 35	U3	U3
SUERC 65995	GC016	30	1865 ± 35	1438 ± 51	U3	U3
SUERC 65994	GC020	9	683 ± 35	357 ± 44	U3	U3
SUERC 65993	GC020	19	3067 ± 37	2864 ± 57	U3	U3
AA-48106	GC020	126	11652 ± 74	13160 ± 90	U2	U2/U1
AA-51569	GC023	30	340 ± 60	64 ± 51	U3	U3
SUERC-681	GC023	49	1215 ± 47	788 ± 58	U3	U3
SUERC-677	GC023	58	1322 ± 43	886 ± 55	U3	U3
AA-51570	GC023	73	1430 ± 55	1011 ± 66	U3	U3
SUERC-679	GC023	111.5	1695 ± 57	1274 ± 59	U2	U3
SUERC-680	GC023	250	2180 ± 61	1801 ± 80	U2	U3
CAMS-82821	GC023	286	2425 ± 40	2099 ± 70	U2	U3
UL 2853	MD04-2833	745	14420 ± 210	17041 ± 312	U1	U1

Table. 3 Sediment volume calculated as the mean of the three numerical integration algorithms; the error is reported as relative standard deviation (%RSD) which integrates the uncertainty in the seismic interpolation and the standard deviation of the numerical integration algorithms. The data is reported for the post-glacial (PG) and glacial (G) sediment at the basin level.

Basin	**Layer**	**Volume**	
		Mean (m^3)	%RSD
Inner	PG	2869825.90	6.48
	G	1301836.56	1.89
Middle	PG	23046267	7.26
	G	7363034.04	1.89
Outer	PG	13371884	7.90
	G	2667373.2	1.89
Loch Sunart	PG	530872293	7.39
	G	599731882	1.89
	Total	**1130604175.55**	**3.61**

Table. 4 Mass of sediment held within Loch Sunart and the mass of total carbon (TC), organic carbon (OC) and inorganic carbon (IC) held within Loch Sunart's postglacial (PG) and glacial (G) sediment.

Basin	Layer	Mass (Mt)	TC (Mt)	OC (Mt)	IC (Mt)
Inner	PG	27.1 ± 3.0	1.3 ± 0.2	1.1 ± 0.1	0.3 ± 0.2
	G	126.7 ± 7.2	0.8 ± 0.6	0.2 ± 0.2	0.6 ± 0.4
Middle	PG	421.5 ± 7.3	14.1 ± 0.3	7.1 ± 0.3	7.0 ± 0.2
	G	738.3 ± 9.6	4.0 ± 0.9	1.2 ± 0.3	2.8 ± 0.6
Outer	PG	203.5 ± 11.1	4.5 ± 0.3	1.3 ± 0.1	3.2 ± 0.2
	G	411.2 ± 9.8	2.2 ± 0.8	0.7 ± 0.1	1.6 ± 0.6
Loch Sunart	PG	652.1 ± 6.6	19.9 ± 0.3	9.4 ± 0.2	10.1 ± 0.2
	G	1276.2 ± 8.9	7.0 ± 0.8	2.1 ± 0.3	4.9 ± 0.6
	Total	**1928.3 ± 7.3**	**26.9 ± 0.5**	**11.5 ± 0.2**	**15.0 ± 0.4**

Table. 5 The effective C storage (C_{eff}) of Loch Sunart's postglacial and glacial sediment in comparison to Scottish terrestrial C stores.

C Inventories	Area (km^2)	TC (Mt)	C_{eff} (Mt km^{-2})	OC_{eff} (Mt km^{-2})	IC_{eff} (Mt km^{-2})	Reference
			Postglacial			
Inner Basin	5.5	1.3	0.238	0.191	0.047	
Middle Basin	24.7	14.1	0.570	0.285	0.284	
Outer Basin	17.1	4.5	0.263	0.077	0.184	
			Glacial			
Inner Basin	5.5	0.8	0.147	0.044	0.104	
Middle Basin	24.7	4.0	0.161	0.047	0.113	
Outer Basin	17.1	2.2	0.129	0.038	0.091	
Postglacial	47.3	19.9	0.412	0.199	0.213	
Glacial	47.3	7.0	0.148	0.044	0.104	
Loch Sunart	47.3	26.9	0.560	0.242	0.318	
			2 m Depth			
Peatlands*	17270	1620		0.094		Chapman et al., 2009
Organo-Mineral Soil*		754				Bradley et al., 2005
Mineral Soil*		498				
			1 m Depth			
Peat	17369	813.9		0.047		Aitkenhead and Coull ,2016
Alluvial Soil	1657	40.8		0.025		
Alpine Soil	3825	145.7		0.038		
Bare Ground	1672	50.5		0.030		
Brown Earth	15971	590.3		0.037		
Gley	15963	645.4		0.040		
Podzol	18159	536.6		0.029		
Ranker	2531	82.6		0.033		
Regosol	437	19.0		0.044		

*****Both studies calculated the soil C stocks excluding IC data therefore the stocks only represent the OC held within these stocks.

Table. 6. Sedimentation, OC accumulation and OC burial rates for Loch Sunart in in comparison to global fjords.

Location	Area (km^2)	SR ($cm\ yr^{-1}$)	OC Accumulation Rate ($g\ m^{-2}\ y^{-1}$)		OC Burial Rate ($g\ m^{-2}\ y^{-1}$)		OC Burial ($Tonnes\ yr^{-1}$)		Reference
			Min	Max	Min	Max	Min	Max	
Loch Sunart	47.3	0.017-0.089	3.0	32.1	1.89[a]	25.68[b]	8.9×10^1	1.2×10^3	This Study
NW Europe/Artic									
Loch Creran	13.3	0.2-0.5			21.9	193.45	2.9×10^2	2.6×10^3	Loh et al., 2008
Nordasvannet Fjord	4.6				2.2		1.0×10^1		Winkelmann and Knies 2005
Storfjord	1424				21.0	40.0	3.0×10^5	5.7×10^5	Müller. 2001
	9								
Kongsfjorden	817				9	13	7.4×10^3	1.0×10^4	Kulinski et al., 2014
Canada/Alaska									
Saguenay Fjord	360				24.5	291.0	8.8×10^3	1.0×10^5	St-Onge and Hillaire-Marcel. 2001
Vegetated Alaskan Fjords					13	82			Cui et al., 2016
Glaciated Alaskan Fjords					30	1113	5.7×10^5	7.6×10^5	
Chile									
Jacaf Fjord	236	0.28	33.4	40.8	21.0	25.7	5.0×10^3	6.1×10^3	Sepúlveda et al., 2011
Ventisquero Sound	7.2	0.74	69.3	82.5	43.7	52.0	3.1×10^2	3.7×10^2	
Puyuhuapi Fjord	111	0.25	11.0	34.2	6.9	21.6	$3.1 \times 1\ 0^3$	9.6×10^3	
Aysen Fjord	340	0.24	10.5	20.7	6.6	13.1	2.3×10^3	4.4×10^3	
Quitralco Fjord	116	0.47	4.6	55.3	2.9	34.8	3.3×10^2	4.0×10^3	
Cupquelan Fjord	125	0.14	1.9	8.4	1.2	5.3	1.5×10^2	6.6×10^2	
New Zealand									
Milford Sound	25.3	0.268	23.2		18.6		4.7×10^2		Knudson et al., 2011
George Sound	32.9	0.087	3.63		2.90		9.5×10^1		
Thompson Sound	49.3	0.113	10.6		8.48		4.18×10^2		
Nancy Sound	13.9	0.204	32.6		26.1		3.62×10^2		Pickrill. 1993
Doubtful Sound	83.7	0.079	23.2		18.6		1.6×10^3		Smith et al., 2015
Breaksea Sound	61.5	0.038	9.07		7.26		4.5×10^2		
Dusky Sound	181	0.012	2.31		1.85		3.3×10^2		
Long Sound	93	0.094	16.0		12.8		1.2×10^3		
Dusky Sound	181	0.16	44	68	35.2[b]	54.4[b]	6.4×10^3	9.8×10^3	Hinojosa et al., 2014
Doubtful Sound	83.7	0.38	115	169	92[b]	135.2[b]	7.7×10^3	1.1×10^4	
George Sound	32.9	0.10	4.8		3.84[b]		1.3×10^2		
Thompson Sound	49.3	0.06-0.17	15.2		12.16[b]		6.0×10^2		

[a]OC Burial rate calculated assuming a burial efficiency of 63% (Sepúlveda et al., 2005).

[b]OC Burial rate calculated assuming a burial efficiency of 80% (Smith et al., 2015).

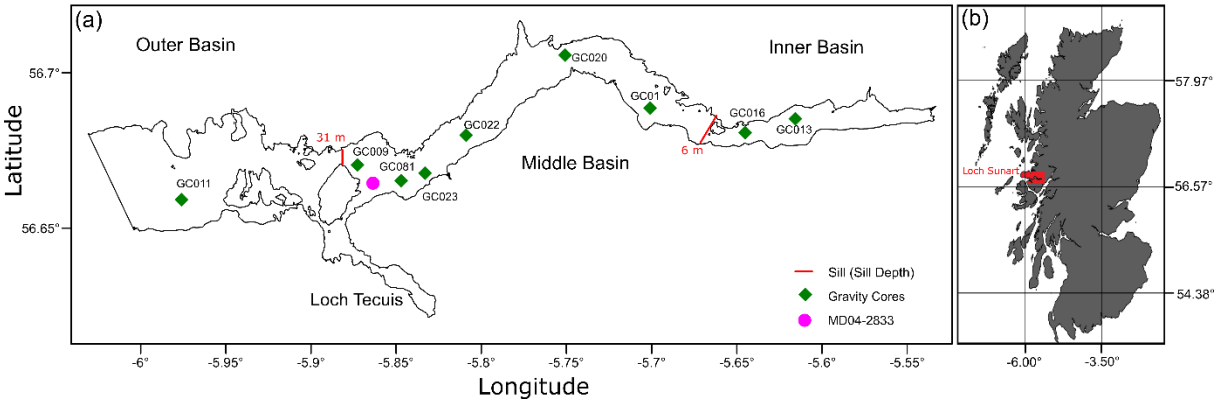

Figure. 1. Maps of Loch Sunart illustrating (a) the three basins and the sediment core locations (b) Loch Sunart in a Scottish context.

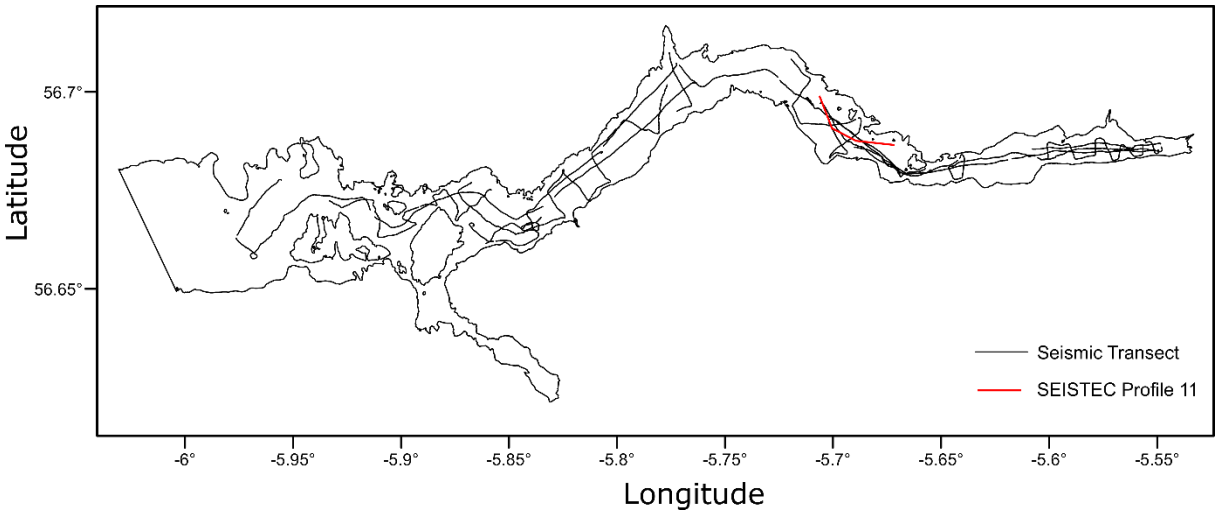

Figure. 2. Map of the 34 Seismic transects undertaken in Loch Sunart with Siestec Profile 11 highlighted.

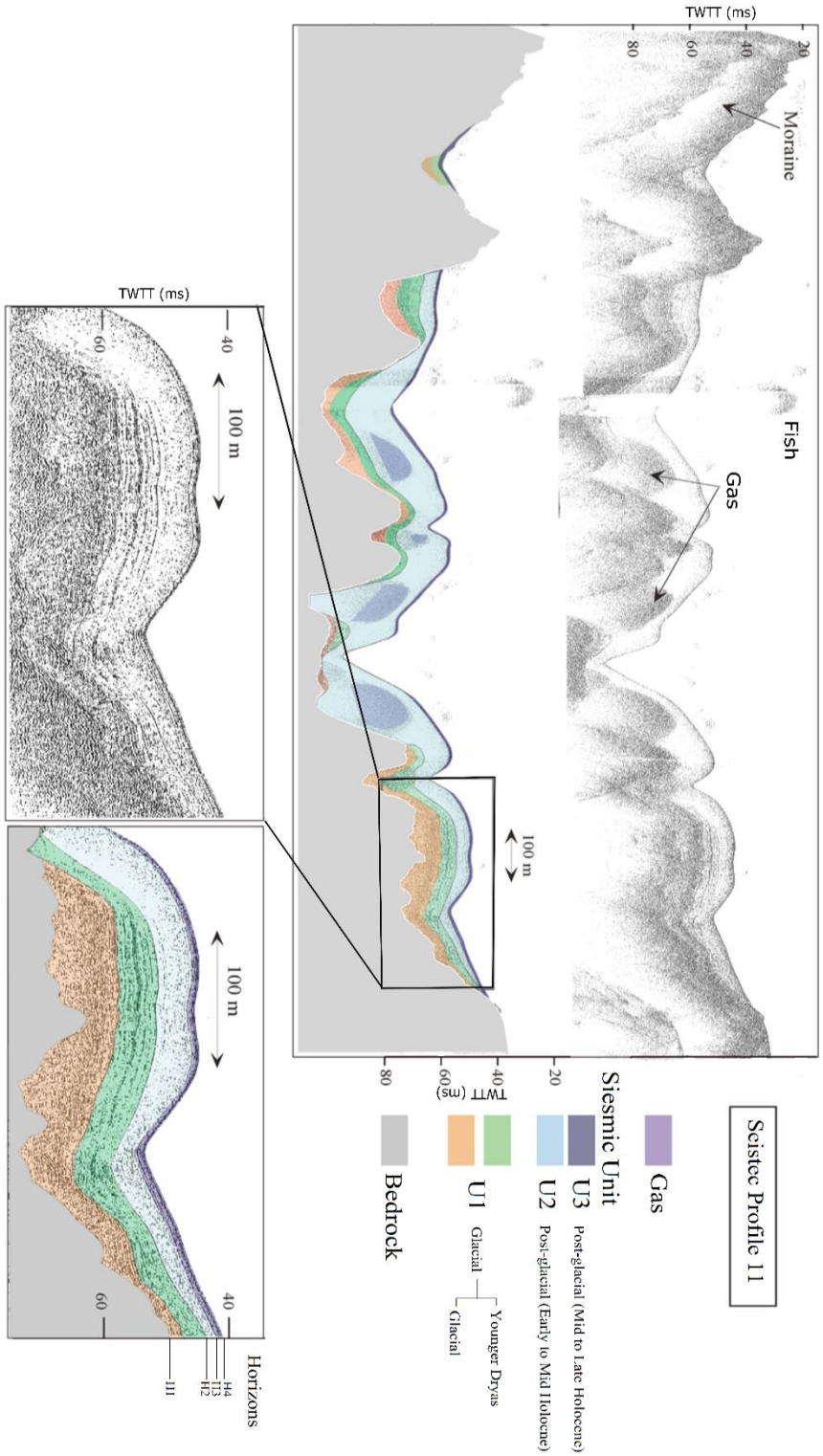

Figure. 3. SIESTEC Profile 11: A characteristic seismic profile displaying the four seismic horizons (H1, H2, H3 and H4) and the three seismic units (U1, U2 and U3) adapted from Baltzer et al.,2010.

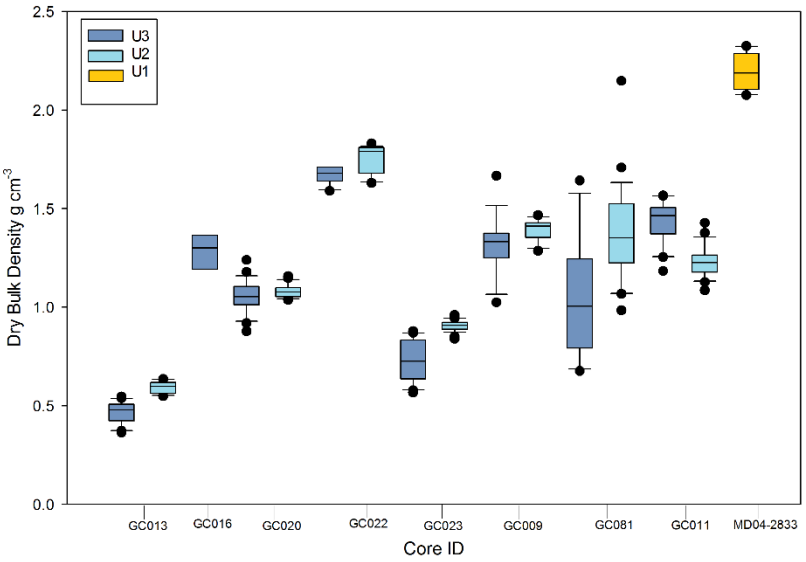

Figure. 4. Dry bulk density values from each sediment cores corresponding to seismic units 1, 2 and 3.

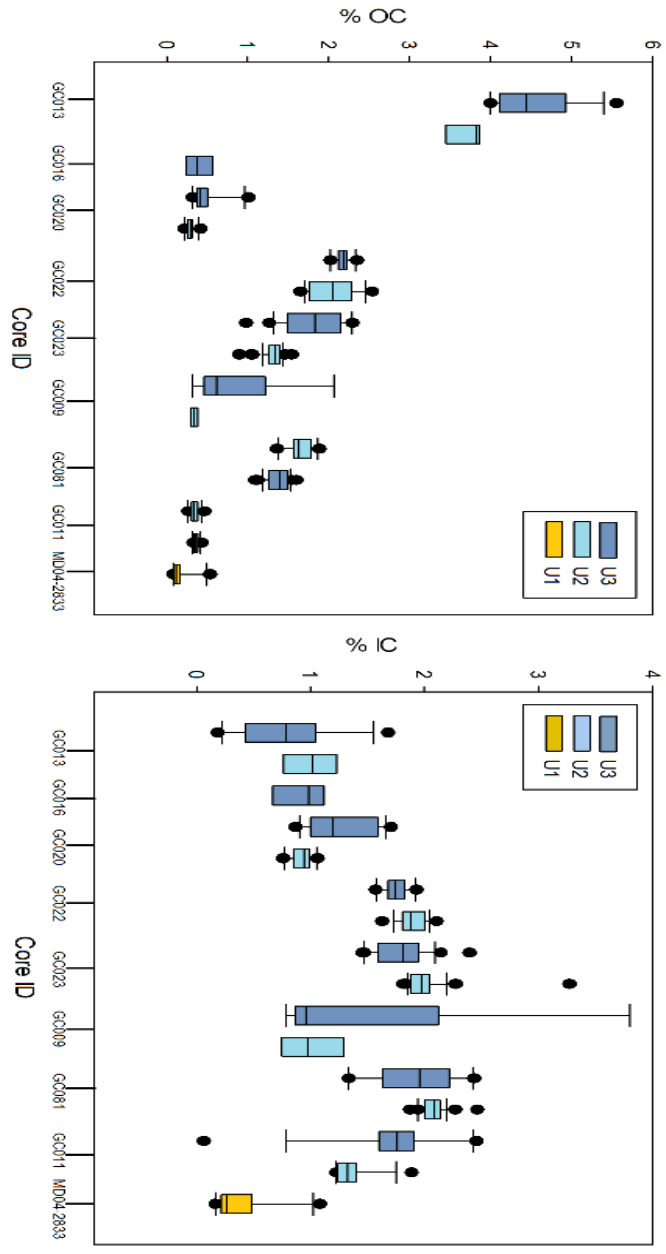

1

2 **Figure. 5.** %OC and %IC values from each sediment cores corresponding to seismic units 1,

3 2 and 3.

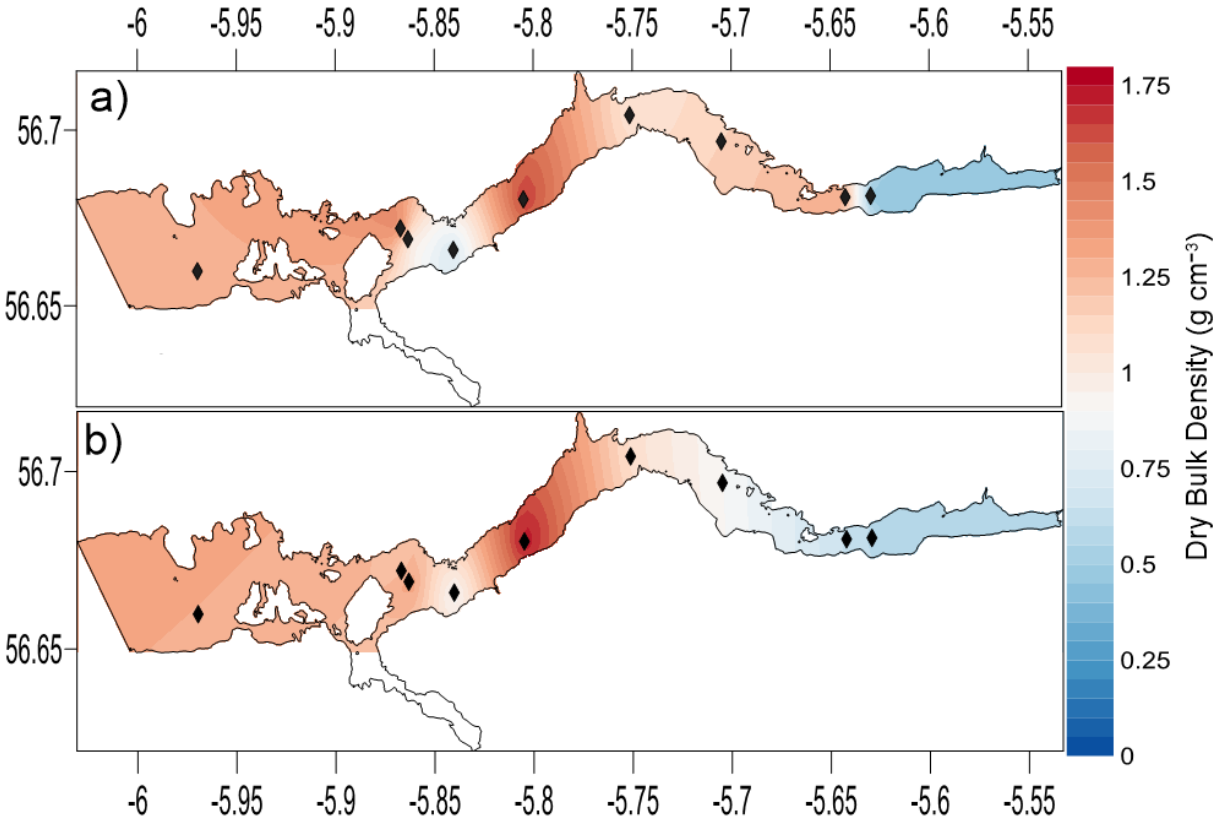

Figure. 6. Contour maps showing the output of the spatial distribution model for the mean dry bulk density of **(a)** U3. **(b)** U2. Sampling locations indicated with black diamonds.

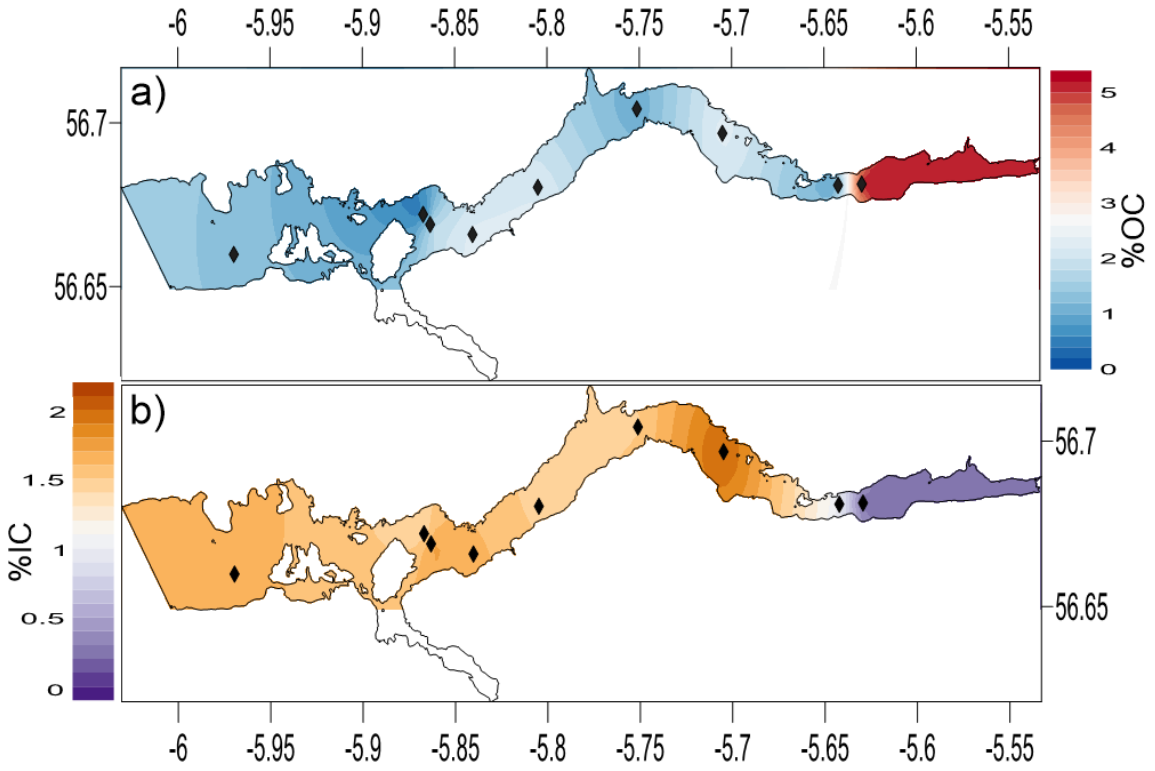

Figure. 7. Output of U3 spatial distribution model for **(a)** Organic carbon. **(b)** Inorganic carbon. Sampling locations indicated with black diamonds.

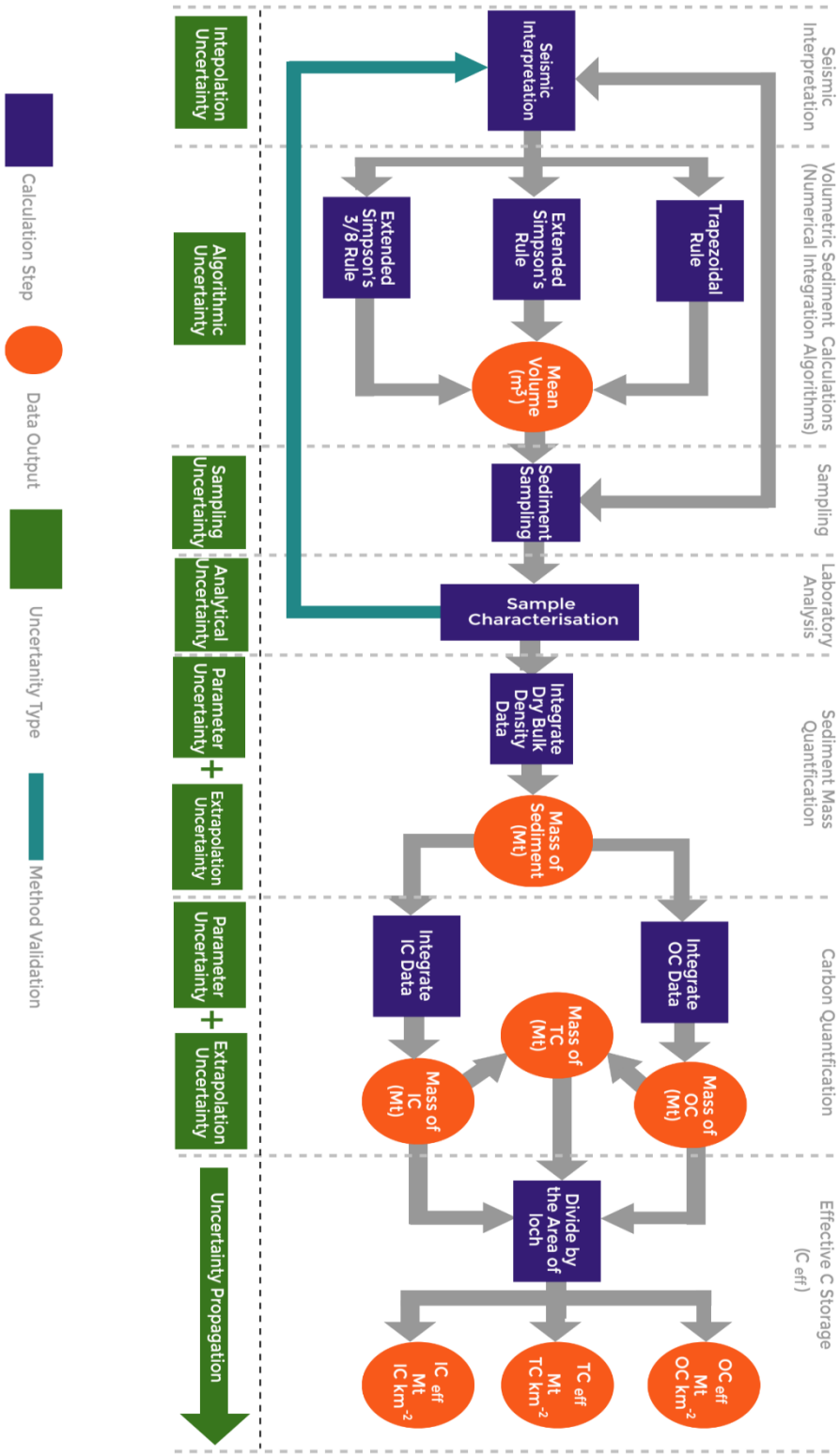

Figure. 8. Flow diagram detailing the steps towards calculating the sedimentary C stocks within a fjord with the known uncertainties specified.